

Effective light-induced Hamiltonian for atoms with large nuclear spin

D. Burba,¹ H. Dunikowski,² M. Robert-de-Saint-Vincent,³ E. Witkowska,² and G. Juzeliūnas¹

¹*Institute of Theoretical Physics and Astronomy, Vilnius University, Saulėtekio 3, LT-10257, Vilnius, Lithuania*

²*Institute of Physics PAS, Aleja Lotników 32/46, 02-668 Warszawa, Poland*

³*Laboratoire de Physique des Lasers, CNRS UMR 7538, Université Sorbonne Paris Nord, F-93430, Villetaneuse, France*

(Dated: October 8, 2024)

Ultra-cold fermionic atoms, having two valence electrons, exhibit a distinctive internal state structure, wherein the nuclear spin becomes decoupled from the electronic degrees of freedom in the ground electronic state. Consequently, the nuclear spin states are well isolated from the environment, rendering these atomic systems an opportune platform for quantum computation and quantum simulations. Coupling with off-resonance light is an essential tool to selectively and coherently manipulate the nuclear spin states. In this paper, we present a systematic derivation of the effective Hamiltonian for the nuclear spin states of ultra-cold fermionic atoms due to such an off-resonance light. We obtain compact expressions for the scalar, vector and tensor light shifts taking into account both linear and quadratic contributions to the hyperfine splitting. The analysis has been carried out using the Green operator approach and solving the corresponding Dyson equation. Finally, we analyze different scenarios of light configurations which lead to the vector- and tensor-light shifts, as well as the pure spin-orbit coupling for the nuclear spin.

I. INTRODUCTION

Alkaline earth atoms stand as a prime platform for the realms of quantum simulation and computation, as well as for high-performance optical clocks [1–7]. These atoms have two valence electrons forming a closed shell ns^2 with zero spin and angular momentum quantum numbers ($S = L = J = 0$) in the electronic ground state 1S_0 . They are also characterized by forbidden optical transitions to electronic triplet states 3P_j , with $j = 0, 1, 2$. Fermionic isotopes possess a nuclear spin that is highly isolated from the environment rendering them a convenient platform for the applications mentioned above [1–7]. The most notable alkaline-earth species are Mg, Ca, Sr, but other species - in particular Yb, and the group IIB transition metals (Hg [8], Cd [9], Zn [10]) share these properties [11–13]. All of them but Zn have been laser-cooled and trapped in the ground state. It is noteworthy that the number of nuclear spin states of their fermionic isotopes can be quite large, such as $N = 10$ for ^{87}Sr , providing beneficial features useful for quantum simulation and computation [6]. The nuclear spin in these atoms thus represents a convenient carrier of quantum information taking into account the long coherence times and the ability of coherent spin control with magnetic and optical fields.

Manipulation of atomic spin states by off-resonant laser fields was studied extensively in the context of both the alkali [14–18] and alkaline earth atoms [6, 7]. The light-induced effective atomic spin Hamiltonian can be generally cast in terms of components known as the scalar, vector and tensor light shifts [16, 17].

Typically, the evaluation of these light shifts involves numerical summation over transitions to various excited states, with differing strengths expressed using e.g. Clebsch-Gordan coefficients [16, 17]. Simple analytical forms of the effective Hamiltonian and the scalar, vector and tensor components of the light shifts are desired

to ease practical experimental implementations and theoretical understanding.

Here we develop a formalism allowing us to obtain compact analytical expressions for the scalar, vector and tensor light shifts of the nuclear spin states for the alkaline-earth-like atoms. We find that the three light shifts are simple rational functions expressed solely in terms of the nuclear spin quantum number, hyperfine splitting energies, and detuning. The method involves the Green operator (the resolvent) approach and the solution of the corresponding Dyson equation, allowing to by-pass explicit analysis of transitions to the specific hyperfine states of the excited state manifold. The technique is related to the one used to analyze the vector light shifts of the alkali atoms presented in Sec. 4 of Ref. [18]. Yet, there are significant differences between the two treatments. In the present analysis of the alkaline-earth-like atoms the electron spin is zero in the ground state, and it is the hyperfine splitting of the excited electronic states which provides the vector and tensor light shifts for the (nuclear) spin states of the ground state atoms. On the other hand, for alkali atoms with a single unpaired outer electron, it is the excited state fine structure splitting which is responsible for the vector light shifts for the spin states in the ground electronic manifold [18]. In our analytical calculations, we have managed to include not only linear but also quadratic terms of the hyperfine coupling operator. Therefore the theory provides a very accurate description of the light shifts for the alkaline-earth-like atoms. To resolve the hyperfine splitting without significant perturbation by spontaneous emission we consider the light shifts due to the 3P_1 intercombination line characterized by a relatively large frequency of the hyperfine splitting A_{HF} and a comparatively small spontaneous emission rate Γ . As an example, for ^{87}Sr atoms $A_{\text{HF}}/2\pi$ is around 2.6×10^5 kHz, whereas $\Gamma/2\pi$ is of the order of 10 kHz [19] for the 3P_1 line. This allows an efficient light-induced manipulation of the nuclear spin states with

minimum decoherence. In the subsequent text, we will consider ^{87}Sr as a typical example. Nevertheless, our analytical findings are broad-reaching and can be applied to other alkaline earth (or alkaline earth-like) atoms with the same structure.

The paper is organised as follows. In Section II we introduce the fine and hyperfine structures of alkali earth or alkali earth-like atoms. Next, in Section III, we present our theory for the derivation of effective Hamiltonian describing the spin ground-state manifold when an atom is coupled with laser radiation. In Section IV, we discuss typical examples of light configuration and the resulting atom-light coupling Hamiltonian, as well as prospects for the realization of spin-orbit coupling for fermionic atoms with nuclear spin. Finally, the concluding Section V summarizes our findings.

II. MANIFOLDS OF GROUND AND EXCITED STATES FOR ALKALINE-EARTH-LIKE ATOMS

We will consider the optical control of nuclear spin for alkali earth or alkali earth-like atoms with two s -shell valence electrons characterised by a nuclear spin i_I . We will study the fermionic isotopes which have non-zero nuclear spin. Bosonic alkaline-earth-like atoms possess zero nuclear spin, as they contain an even number of protons and even number of neutrons. Thus the bosonic species are not of interest for the present analysis of the manipulation of atomic nuclear spin.

In the ground electronic manifold denoted by 1S_0 the spins of outer electrons of alkali earth-like atoms form a singlet, so the quantum numbers of the electronic spin \mathbf{S} and the orbital angular momenta \mathbf{L} are zero, as well as the total electronic momentum $\mathbf{J} = \mathbf{L} + \mathbf{S}$, namely $s = l = j = 0$. It is a reason why the fine and hyperfine couplings are not affecting the ground electronic state. The energy of this state is taken to be zero $E_g = 0$.

The excited electronic state of interest $|j, m_j\rangle$ with $j = 0, 1, 2$ belongs to the manifold 3P_j where spins of the outer electrons form a triplet, and the state of the atom is characterized by the spin and orbital angular momentum quantum numbers, $s = 1$ and $l = 1$, respectively¹. The state $|j, m_j\rangle$ is an eigenstate of \mathbf{S}^2 , \mathbf{L}^2 , \mathbf{J}^2 and \mathbf{J}_z with the corresponding eigenvalues $\hbar^2 s(s+1) = 2\hbar^2$, $\hbar^2 l(l+1) = 2\hbar^2$, $\hbar^2 j(j+1)$ and $\hbar m_j$. Without including the fine and hyperfine couplings the excited state is degenerate concerning j . The fine structure coupling removes this degeneracy.

The fine structure (FS) coupling between the total electron spin and orbital angular momentum is

described by the Hamiltonian $H_{\text{FS}} = \frac{A_{\text{FS}}}{\hbar} \mathbf{L} \cdot \mathbf{S} = \frac{A_{\text{FS}}}{\hbar} (\mathbf{J}^2 - \mathbf{L}^2 - \mathbf{S}^2) / 2$ providing j -dependent energies $E_{\text{FS}}^{(j)} = \hbar A_{\text{FS}} [j(j+1) - 4] / 2$ for $l = s = 1$. Therefore, one has

$$E_{\text{FS}}^{(j=0)} = -2\hbar A_{\text{FS}}, \quad E_{\text{FS}}^{(j=1)} = -\hbar A_{\text{FS}}, \quad E_{\text{FS}}^{(j=2)} = \hbar A_{\text{FS}}. \quad (1)$$

The state with $j = 2$ is not accessible via the dipole transitions from the ground state manifold 1S_0 with $j = 0$, and thus will not be considered by us in the further part of the text. The transition to the state with $j = 0$, also known as "clock transition", is double forbidden, both by spin and orbital degrees of freedom. It is very weak, and only relevant if the radiation frequency is very close to this state's resonance. Therefore, in what follows, we will consider only the transition to the excited state manifold 3P_1 corresponding to $j = 1$. This transition called the intercombination line, is forbidden by spin flip, but opens due to $j - j$ coupling admixing with the 1P_1 state [20].

The hyperfine (HF) coupling between the total electronic angular momentum \mathbf{J} and the nuclear spin \mathbf{I} is generally given by the Hamiltonian (see e.g. ref. [17]):

$$H_{\text{HF}} = \frac{A'_{\text{HF}}}{\hbar} \mathbf{I} \cdot \mathbf{J} + B_{\text{HF}} \frac{6(\mathbf{I} \cdot \mathbf{J})^2 + 3\hbar^2 \mathbf{I} \cdot \mathbf{J} - 2\mathbf{I}^2 \mathbf{J}^2}{4\hbar^3 i_I (2i_I - 1) j (2j - 1)}, \quad (2)$$

where in the present situation $j = 1$. Here A'_{HF} and B_{HF} are HF constants. In the case of strontium atoms, their values are $A'_{\text{HF}}/2\pi = -260085 \pm 2 \text{ kHz}$ and $B_{\text{HF}}/2\pi = -35667 \pm 21 \text{ kHz}$ [19, 21]. It is convenient to represent H_{HF} as

$$H_{\text{HF}} = \frac{A_{\text{HF}}}{\hbar} \left[\mathbf{I} \cdot \mathbf{J} + \frac{\gamma}{\hbar^2} (\mathbf{I} \cdot \mathbf{J})^2 \right], \quad (3)$$

where $A_{\text{HF}} = A'_{\text{HF}} + 3B_{\text{HF}}/[4i_I(2i_I - 1)j(2j - 1)]$, and the dimensionless parameter $\gamma = 6B_{\text{HF}}/[A_{\text{HF}}4i_I(2i_I - 1)j(2j - 1)]$ describing a relative strength of the quadratic term is generally much less than the unity. For ^{87}Sr atoms one has $\gamma \approx 0.006$, and we will use this value in specific examples. In Eq. (3) a uniform shift of energy proportional to $\mathbf{I}^2 \mathbf{J}^2$ has been incorporated to the excitation energy $E_{\text{FS}}^{(j=1)}$, whereas the two terms of Eq. (2) proportional to $\mathbf{I} \cdot \mathbf{J}$ have been merged to a single term characterised by the modified frequency A_{HF} .

The eigenstates of hyperfine Hamiltonian are also eigenstates of \mathbf{F}^2 ($\mathbf{F} = \mathbf{I} + \mathbf{J}$), \mathbf{I}^2 , \mathbf{J}^2 and \mathbf{F}_z , and the corresponding eigenvalues are $\hbar^2 f(f+1)$, $\hbar^2 i_I(i_I+1)$, $\hbar^2 j(j+1)$, and $\hbar m_f$. For the excited state 3P_1 manifold of interest one has $j = 1$, so f can take the values $f = i_I$ and $f = i_I \pm 1$. The energies of these excited states are:

$$E_{i_I+1} = \hbar A_{\text{HF}} i_I (1 + \gamma i_I), \quad (4)$$

$$E_{i_I} = -\hbar A_{\text{HF}} (1 - \gamma), \quad (5)$$

$$E_{i_I-1} = -\hbar A_{\text{HF}} (i_I + 1) [1 - \gamma (i_I + 1)]. \quad (6)$$

The hyperfine structure for the electronic line 3P_1 is schematically represented in Fig. 1.

¹ Alternatively, the theory presented here is also applicable for virtual transitions via the 1P_1 manifold. However, we will concentrate on the 3P_1 manifold, as its higher ratio between hyperfine structure and linewidth makes it more relevant experimentally due to much smaller rate of spontaneous emission.

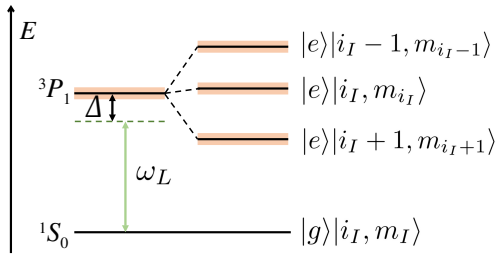


FIG. 1. A sketch of the atomic levels for alkali-like atoms illustrating the hyperfine structure of the excited electronic line 3P_1 . The order of the excited states depends on the sign of A_{HF} ; here we take $A_{\text{HF}} < 0$ as in ${}^{87}\text{Sr}$. The probe frequency ω_L is tuned in a vicinity of the transition ${}^1S_0 \rightarrow {}^3P_1$ manifold with the detuning Δ .

III. EFFECTIVE HAMILTONIAN

We consider the effects of light field \mathbf{E} on atomic nuclear spin states in the ground electronic manifold 1S_0 due to the virtual transition to the excited state manifold 3P_1 . In the dipole approximation, the interaction between a monochromatic light field characterized by the electric field strength \mathbf{E} and an atom can be described by the operator

$$V = -\mathbf{d} \cdot \mathbf{E} = -\sum_q d_q \tilde{\mathcal{E}}_q \cos(\phi_q - \omega_L t). \quad (7)$$

where the components of the electric field amplitude $\tilde{\mathcal{E}}_q$ and phase ϕ_q of the radiation are generally position dependent. Here $\mathbf{d} = -e \sum_{\alpha} \mathbf{r}_{\alpha}$ is the electric dipole operator, e is an electron charge and \mathbf{r}_{α} is the position of the α th electron within the atom.

We will go to the frame rotated at the driving frequency ω_L and subsequently apply the rotating wave approximation (RWA) by removing terms oscillating at frequencies $\omega_L, 2\omega_L$ in the transformed interaction Hamiltonian which then takes the form, see e.g. Chapter 4 of Ref. [18]:

$$V = -\frac{1}{2} \sum_q [\mathcal{E}_q^* P_g d_q P_e + \mathcal{E}_q P_e d_q P_g], \quad (8)$$

where we introduced the complex electric field $\mathcal{E}_q = \tilde{\mathcal{E}}_q e^{i\phi_q}$.

In the above formula, P_g and P_e are projector operators onto the ground and excited state manifolds 1S_0 and 3P_1 , respectively.

A. Analysis of effective Hamiltonian

If the incident light \mathcal{E} with components \mathcal{E}_q is sufficiently weak and/or well detuned from atomic resonances, the saturation parameter is small, and the atom-light interaction effectively provides coupling between the

nuclear spin states $|i_I, m_{i_I}\rangle$ of the electronic ground state $|g\rangle$ via virtual transitions to the excited states without populating them². Specifically, the adiabatic elimination of the excited states can be described in the second order (with respect to the interaction V) via Schrieffer-Wolff transformation, see e.g. Supplementary Materials of [22]. This provides the corresponding second order effective atomic Hamiltonian for the ground state manifold:

$$\hat{H}_{\text{eff}} = P_g V G V P_g \quad (9)$$

where

$$G = (\Delta - H_{\text{HF}})^{-1} \quad (10)$$

is the Green operator and $\Delta = E_{\text{FS}}^{(j=1)} - E_g - \hbar\omega_L$ is the detuning. Although our analysis is perturbative to second order in electron-light interaction V , the hyperfine interaction H_{HF} is treated exactly. Note that by adding an imaginary part to the detuning Δ , one can include effects of losses due to spontaneous emission. This is discussed in Sec. III B.

The effective atomic Hamiltonian can be expressed as

$$\hat{H}_{\text{eff}} = \frac{1}{4} \mathcal{E}_s^* D_{s,q} \mathcal{E}_q. \quad (11)$$

Here and below the summation over repeated indices of vectors and tensors is assumed. In Eq.(11) we introduced the tensor operator acting on the ground state manifold:

$$D_{s,q} = P_g d_s P_e G P_e d_q P_g, \quad (12)$$

where the Green operator G obeys a Dyson-type equation (identity)

$$G = \frac{1}{\Delta} + \frac{1}{\Delta} H_{\text{HF}} G, \quad (13)$$

see Appendix A. Combining Eqs. (12) and (13), one has

$$D_{s,q} = \frac{|d_{ge}^2|}{\Delta} P_g \delta_{sq} + \frac{1}{\Delta} P_g d_s P_e H_{\text{HF}} G P_e d_q P_g, \quad (14)$$

where

$$|d_{ge}^2| = \frac{1}{3} \langle g | d_q P_e d_q | g \rangle \quad (15)$$

characterizes the strength of the dipole transition and equals to the third of the reduced matrix element $\langle g | d_q P_e d_q | g \rangle = \sum_e |\langle e | d_q | g \rangle|^2$. The dipole transition is weak, but non-zero. This is because the excited state manifold 3P_1 contains a small admixture of the manifold

² This means we are not considering the resonant regime ($|\Delta - E_f| \lesssim |d_{ge}\mathbf{E}|$), where E_f is energy of hyperfine state, given by Eqs. (4)-(6) and $|d_{ge}| = \sqrt{|d_{ge}^2|}$ is defined in Eq. (15). In the resonant situation one would have a significant excited state population and observe Rabi oscillations.

1P_1 with the same $j = 1$, but zero spin $s = 0$, and the transitions to the latter manifold $^1S_0 \rightarrow ^1P_1$ are dipole allowed.

According to the Landé projection theorem [16], the effective Hamiltonian (11) can be represented in the form

$$\hat{H}_{\text{eff}} = \frac{b_0}{4} (\boldsymbol{\mathcal{E}}^* \cdot \boldsymbol{\mathcal{E}}) + i \frac{b_1}{4\hbar} \mathbf{I} \cdot (\boldsymbol{\mathcal{E}}^* \times \boldsymbol{\mathcal{E}}) + \frac{b_2}{4\hbar^2} \left[(\boldsymbol{\mathcal{E}}^* \cdot \mathbf{I}) (\boldsymbol{\mathcal{E}} \cdot \mathbf{I}) - \frac{1}{3} |\boldsymbol{\mathcal{E}}|^2 \mathbf{I}^2 + \text{h.c.} \right]. \quad (16)$$

where the coefficients b_0, b_1 and b_2 characterize the strengths of the scalar, vector and tensor terms. Conventionally the effective Hamiltonian is calculated using the explicit expressions for the transition matrix elements involving the Clebsch-Gordon coefficients. Here, we perform analytical calculations of the coefficients b_0, b_1 and b_2 defining the effective Hamiltonian to derive their simple forms in a self-consistent way based on solution of Eq. (14) for $D_{s,q}$. To this end, it is convenient to introduce a vector operator \mathbf{K} with Cartesian components derived from $D_{s,q}$:

$$K_s = D_{s,q} \mathcal{E}_q. \quad (17)$$

In terms of \mathbf{K} , the effective Hamiltonian of Eq (11) reads:

$$\hat{H}_{\text{eff}} = \frac{1}{4} \boldsymbol{\mathcal{E}}^* \cdot \mathbf{K}. \quad (18)$$

Multiplying Eq. (14) by \mathcal{E}_q from the right-hand side, we write down the relation for the vector-operator \mathbf{K}

$$\mathbf{K} = \frac{1}{\Delta} P_g |d_{ge}^2| \boldsymbol{\mathcal{E}} + \frac{A_{\text{HF}}}{\hbar \Delta} P_g \mathbf{d} (\mathbf{I} \cdot \mathbf{J}) \left(1 + \frac{\gamma}{\hbar^2} \mathbf{I} \cdot \mathbf{J} \right) G P_e (\mathbf{d} \cdot \boldsymbol{\mathcal{E}}) P_g. \quad (19)$$

As demonstrated in Appendix B1, this provides the following equation for \mathbf{K} :

$$\eta \mathbf{K} = \frac{1}{\Delta} P_g |d_{ge}^2| \boldsymbol{\mathcal{E}} + i \frac{A_{\text{HF}}}{\Delta} (1 - \gamma) (\mathbf{I} \times \mathbf{K}) - \gamma \frac{A_{\text{HF}}}{\hbar \Delta} \mathbf{I} (\mathbf{I} \cdot \mathbf{K}), \quad (20)$$

where $\eta = 1 - \gamma A_{\text{HF}} \hbar i_I (i_I + 1) / \Delta$.

Anticipating the effective Hamiltonian of the form (16), we will look for the following \mathbf{K} ansatz

$$\mathbf{K} = \left[a_0 \boldsymbol{\mathcal{E}} - i \frac{a_1}{\hbar} \mathbf{I} \times \boldsymbol{\mathcal{E}} + \frac{a_2}{\hbar^2} \mathbf{I} (\mathbf{I} \cdot \boldsymbol{\mathcal{E}}) \right] P_g, \quad (21)$$

where a_0, a_1 and a_2 are real coefficients. Inserting the ansatz (21) into Eq. (20), one gets a system of equations for these coefficients, giving

$$a_0 = - \frac{|d_{ge}^2|}{\hbar A_{\text{HF}}} \frac{\bar{E}^{(+)}}{(\bar{\Delta} - \bar{E}_{i_I+1}) (\bar{\Delta} - \bar{E}_{i_I-1})}, \quad (22)$$

$$a_1 = \frac{|d_{ge}^2|}{\hbar A_{\text{HF}}} \frac{\bar{E}_{i_I}}{(\bar{\Delta} - \bar{E}_{i_I+1}) (\bar{\Delta} - \bar{E}_{i_I-1})}, \quad (23)$$

$$a_2 = \frac{|d_{ge}^2|}{\hbar A_{\text{HF}}} \frac{\gamma \bar{E}^{(-)} - \bar{E}_{i_I}^2}{(\bar{\Delta} - \bar{E}_{i_I+1}) (\bar{\Delta} - \bar{E}_{i_I}) (\bar{\Delta} - \bar{E}_{i_I-1})}, \quad (24)$$

with

$$\bar{E}^{(\pm)} = (\bar{E}_{i_I+1} \pm \bar{E}_{i_I} + \bar{E}_{i_I-1}) / 2 - \bar{\Delta}. \quad (25)$$

where $\bar{\Delta} = \Delta / (\hbar A_{\text{HF}})$ and $\bar{E}_f = E_f / (\hbar A_{\text{HF}})$ (with $f = i_I - 1, i_I, i_I + 1$) are, respectively, the dimensionless detuning and energies of hyperfine states, and E_f is defined by Eqs. (4)-(6). Details of derivation are in Appendix B2.

Substituting the solution (21) for \mathbf{K} into Eq. (18), one arrives at the explicit result for the ground state effective Hamiltonian expressed in terms of the coefficients $a_{0,1,2}$

$$\hat{H}_{\text{eff}} = \frac{a_0}{4} (\boldsymbol{\mathcal{E}}^* \cdot \boldsymbol{\mathcal{E}}) + i \frac{a_1}{4\hbar} \mathbf{I} \cdot (\boldsymbol{\mathcal{E}}^* \times \boldsymbol{\mathcal{E}}) + \frac{a_2}{4\hbar^2} (\boldsymbol{\mathcal{E}}^* \cdot \mathbf{I}) (\boldsymbol{\mathcal{E}} \cdot \mathbf{I}), \quad (26)$$

where for brevity we have omitted the ground state projector operator P_g .

Note that the self-consistent method we used to find the vector \mathbf{K} of Eq. (21) can be applied on the level of the tensor $D_{s,q}$ featured in Eqs. (12) and (14). In that case one finds

$$D_{s,q} = a_0 \delta_{sq} + i \frac{a_1}{\hbar} I_k \epsilon_{ksq} + \frac{a_2}{\hbar^2} I_s I_q. \quad (27)$$

This leads to the same form of the effective Hamiltonian (26) with the same coefficients $a_{0,1,2}$ defined by Eqs. (22)-(24).

Using the fact that $\boldsymbol{\mathcal{E}}^* \cdot (\mathbf{I} \times \boldsymbol{\mathcal{E}}) = -\boldsymbol{\mathcal{E}}^* \cdot (\boldsymbol{\mathcal{E}} \times \mathbf{I}) = -(\boldsymbol{\mathcal{E}}^* \times \boldsymbol{\mathcal{E}}) \cdot \mathbf{I}$, we express the effective Hamiltonian (26) in the symmetric and traceless form as in Eq. (16). Consequently, we obtain the following relations for the coefficients b_0, b_1 and b_2 defining the scalar, vector and tensor light shifts

$$b_0 = a_0 + \bar{i}_I^2 a_2 / 3, \quad b_1 = a_1 + a_2 / 2 \quad \text{and} \quad b_2 = a_2 / 2. \quad (28)$$

with

$$\bar{i}_I^2 \equiv \mathbf{I}^2 / \hbar^2 = i_I (i_I + 1), \quad (29)$$

It is convenient to define the dimensionless b coefficients

$$\bar{b}_u = b_u \hbar A_{\text{HF}} / |d_{ge}^2|, \quad \text{with} \quad u = 0, 1, 2. \quad (30)$$

Calling on Eqs. (22)-(24) and (28), one arrives at the explicit expressions for the latter coefficients:

$$\bar{b}_0 = \frac{-3\bar{E}^{(+)} (\bar{\Delta} - \bar{E}_{i_I}) + \bar{i}_I^2 (\gamma \bar{E}^{(-)} - \bar{E}_{i_I}^2)}{3 (\bar{\Delta} - \bar{E}_{i_I+1}) (\bar{\Delta} - \bar{E}_{i_I}) (\bar{\Delta} - \bar{E}_{i_I-1})}, \quad (31)$$

$$\bar{b}_1 = \frac{2\bar{E}_{i_I} (\bar{\Delta} - \bar{E}_{i_I}) + (\gamma \bar{E}^{(-)} - \bar{E}_{i_I}^2)}{2 (\bar{\Delta} - \bar{E}_{i_I+1}) (\bar{\Delta} - \bar{E}_{i_I}) (\bar{\Delta} - \bar{E}_{i_I-1})}, \quad (32)$$

$$\bar{b}_2 = \frac{(\gamma \bar{E}^{(-)} - \bar{E}_{i_I}^2)}{2 (\bar{\Delta} - \bar{E}_{i_I+1}) (\bar{\Delta} - \bar{E}_{i_I}) (\bar{\Delta} - \bar{E}_{i_I-1})}. \quad (33)$$

In Fig. 2 we plot the dimensionless coefficients $\bar{b}_{0,1,2}$ as a function of the relative detuning $\bar{\Delta}$ using Eqs. (31)-(33)

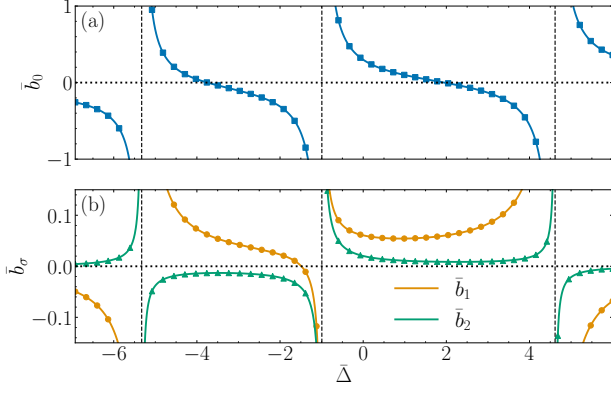


FIG. 2. Dependence of the rescaled scalar \bar{b}_0 (a), vector \bar{b}_1 and tensor \bar{b}_2 coefficients (b) on the rescaled detuning $\bar{\Delta}$ for $i_I = 9/2$ and $\gamma = 0.006$, corresponding to ^{87}Sr atoms. The analytical results given by (31), (32) and (33) are marked by solid lines while squares, circles and triangles, respectively, represent Clebsch-Gordan numerical calculations.

and the conventional Clebsch-Gordan approach outlined in Appendix C. There is a perfect agreement with a relative deviation due to finite computing precision below 10^{-13} .

The analytical expressions (31)-(33) show explicitly the detuning dependence of the coefficients $\bar{b}_{0,1,2}$ describing, respectively, the scalar, vector and tensor light shifts. For example, by taking the ^{87}Sr atom with $i_I = 9/2$ and choosing detuning comparable with the HF energies, $\bar{\Delta} = \sum_{f=i_I, i_I \pm 1} \bar{E}_f/3 \approx -0.57$, the dimensional coefficients are: $b_0 \approx 0.76$, $b_1 \approx 0.09$ and $b_2 \approx 0.05$. Thus the scalar term dominates for the specific value of $\bar{\Delta}$ chosen. Yet by changing $\bar{\Delta}$ it is possible to find a point where the scalar term \bar{b}_0 changes the sign and thus goes through the zero point, as one sees in Fig. 2. Hence one can eliminate the scalar term without cancelling the other terms.

Neglecting the quadratic hyperfine coupling ($\gamma = 0$ and thus $\bar{E}_{i_I} = -1$), Eqs. (32)-(33) shows that the ratio of the vector and tensor light shifts goes linearly with the detuning:

$$\bar{b}_1/\bar{b}_2 = 2\bar{\Delta} + 3. \quad (34)$$

Such a linear dependence holds well also after including the quadratic hyperfine coupling which is typically small ($\gamma \ll 1$). From Eq. (34) it follows that the ratio \bar{b}_1/\bar{b}_2 goes to zero at $\bar{\Delta} = -3/2$ for $\gamma = 0$.

For far-off resonance radiation when detuning is much larger than the energy of the hyperfine splitting $|\bar{\Delta}| \gg 1$, the dimensionless coefficients read up to terms cubic in

detuning

$$\bar{b}_0 \approx \bar{\Delta}^{-1} + \frac{2}{3}\gamma\bar{i}_I^2\bar{\Delta}^{-2} + \frac{2}{3}\bar{i}_I^2 [1 + \gamma(\gamma\bar{i}_I^2 - 1)] \bar{\Delta}^{-3}, \quad (35)$$

$$\bar{b}_1 \approx -\left(1 - \frac{\gamma}{2}\right) \bar{\Delta}^{-2} + \frac{1}{2} [1 - 4\gamma\bar{i}_I^2 + \gamma^2 (3\bar{i}_I^2 - 1)] \bar{\Delta}^{-3}, \quad (36)$$

$$\bar{b}_2 \approx -\frac{\gamma}{2}\bar{\Delta}^{-2} + \frac{1}{2} [-1 + 4\gamma - \gamma^2 (\bar{i}_I^2 + 3)] \bar{\Delta}^{-3}. \quad (37)$$

In this way, for large detuning, $\bar{\Delta} \gg 1$, the scalar light shift $\propto \bar{\Delta}^{-1}$ decreases linearly with the inverse detuning, whereas the vector light shift $\propto \bar{\Delta}^{-2}$ goes quadratically. For intermediate detuning $1 \ll \bar{\Delta} \ll \gamma^{-1}$ the tensor light shift decreases as $\bar{\Delta}^{-3}$ and then cross over to an asymptotic decay $\propto \gamma/\bar{\Delta}^2$ for $\bar{\Delta} \gg \gamma^{-1}$, with $|\bar{b}_2/\bar{b}_1| \ll 1$ ensured by the weaker quadratic hyperfine coupling (typically $\gamma \ll 1$).

B. Effects of spontaneous emission

Let us now include the effects of the finite radiative lifetime of the excited state. This can be done by replacing the detuning Δ by $\Delta - i\hbar\Gamma$ in our treatment including the expressions for the coefficients $a_{0,1,2}$ and $b_{0,1,2}$, where Γ is the excited state linewidth due to spontaneous emission. Consequently, the effective Hamiltonian acquires a non-Hermitian part representing the radiative losses.

To estimate the losses let us expand $\text{Im } \bar{b}_{0,1,2}$ to first order in the linewidth Γ assuming that the detuning is not too close to the hyperfine lines ($|\Delta - E_f| \gg \hbar\Gamma$) and neglecting the quadratic contribution to the hyperfine coupling ($\gamma = 0$):

$$\text{Im } \bar{b}_0 \approx \frac{3(\bar{\Delta} + 1)^4 + 2(\bar{\Delta} + 1)\bar{i}_I^2 + \bar{i}_I^4}{3(\bar{\Delta} - \bar{E}_{i_I+1})^2 (\bar{\Delta} - \bar{E}_{i_I})^2 (\bar{\Delta} - \bar{E}_{i_I-1})^2} \bar{\Gamma}, \quad (38)$$

$$\text{Im } \bar{b}_1 \approx -\frac{4\bar{\Delta}^3 + 13\bar{\Delta}^2 + 12\bar{\Delta} - \bar{i}_I^2 + 3}{2(\bar{\Delta} - \bar{E}_{i_I+1})^2 (\bar{\Delta} - \bar{E}_{i_I})^2 (\bar{\Delta} - \bar{E}_{i_I-1})^2} \bar{\Gamma}, \quad (39)$$

$$\text{Im } \bar{b}_2 \approx -\frac{3\bar{\Delta}^2 + 4\bar{\Delta} - \bar{i}_I^2 + 1}{2(\bar{\Delta} - \bar{E}_{i_I+1})^2 (\bar{\Delta} - \bar{E}_{i_I})^2 (\bar{\Delta} - \bar{E}_{i_I-1})^2} \bar{\Gamma}, \quad (40)$$

with $\bar{\Gamma} = \Gamma/A_{\text{HF}}$.

Although these formulas do not hold when the detuning $|\Delta - E_f|$ becomes comparable to $\hbar\Gamma$ or is smaller, such a situation is not interesting because of a significant increase of losses compared to the light shifts. On the other hand, the intermediate ($\hbar\Gamma \ll |\Delta - E_f| \ll \hbar A_{\text{HF}}$) and far detuned regimes are well described by Eqs. (38)-(40). For the far detuned radiation, $|\Delta - E_f| \gg \hbar A_{\text{HF}}$, the losses go as $\text{Im } \bar{b}_0 \propto \bar{\Delta}^{-2}$, $\text{Im } \bar{b}_1 \propto \bar{\Delta}^{-3}$ and $\text{Im } \bar{b}_2 \propto \bar{\Delta}^{-4}$, so the dominant loss term $\text{Im } \bar{b}_0$ and the vector light shift coefficient $\text{Re } \bar{b}_1$ both go as $1/\bar{\Delta}^2$. Hence, in the far detuned regime the ratio $\text{Im } \bar{b}_0/\text{Re } \bar{b}_1$ becomes constant and

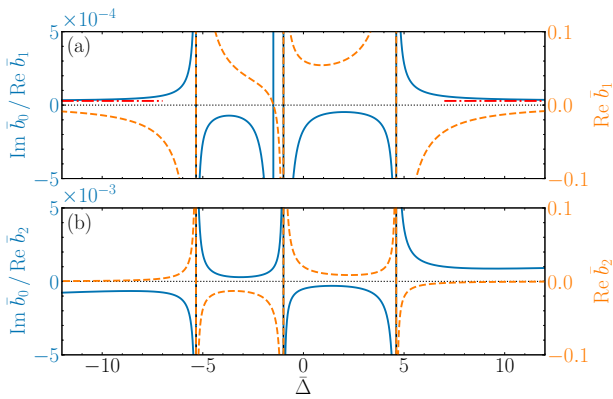


FIG. 3. Dependence of the loss ratio $\text{Im } \bar{b}_0/\text{Re } \bar{b}_{1,2}$ (blue solid lines, left vertical axis) and the dimensionless vector (a) and tensor (b) polarizabilities $\text{Re } \bar{b}_{1,2}$ (dashed yellow lines, the right vertical axis) on the dimensionless detuning $\bar{\Delta}$ for $\Gamma/|A_{\text{HF}}| = 3 \times 10^{-5}$. Red dash-dotted horizontal lines represent the limiting value of the ratio $\text{Im } \bar{b}_0/\text{Re } \bar{b}_1$ for large detuning given by Eq. (41).

is determined by the ratio of the linewidth Γ and the hyperfine structure constant A_{HF} :

$$|\text{Im } \bar{b}_0/\text{Re } \bar{b}_1| \approx \Gamma/|A_{\text{HF}}| \ll 1. \quad (41)$$

For example, for the $^1S_0 \rightarrow ^3P_1$ line of the species: spin-7/2 ^{43}Ca ; spin-9/2 ^{87}Sr ; spin-1/2 ^{171}Yb ; spin-5/2 ^{173}Yb , this ratio is, respectively, $\Gamma/|A_{\text{HF}}| = 2.10^{-6}; 3.10^{-5}; 5.10^{-5}; 2.10^{-4}$, showing that the intercombination line of alkaline-earth-like atoms is very favorable to engineer nuclear-spin-sensitive vector or tensor light shifts.

Yet in the far-detuned regime, the vector and tensor light shifts decrease considerably. To get their larger values, one needs to go closer to the resonances or even between the resonance lines. In that case the relative contribution of the losses can still have reasonably small (of the order of 10^{-4}) with a considerably increase of the vector light polarizability, as one can see in Fig. 3.

IV. SPECIFIC CONFIGURATIONS

The analytical form of the effective Hamiltonian (16) of the ground state manifold, can be presented as

$$\hat{H}_{\text{eff}} = \hat{H}_{\text{eff}(0)} + \hat{H}_{\text{eff}(1)} + \hat{H}_{\text{eff}(2)}, \quad (42)$$

where

$$\hat{H}_{\text{eff}(0)} := \frac{b_0}{4} (\mathcal{E}^* \cdot \mathcal{E}) = \frac{b_0}{4} |\mathcal{E}|^2, \quad (43)$$

is the scalar component,

$$\hat{H}_{\text{eff}(1)} := \frac{ib_1}{4\hbar} \mathbf{I} \cdot (\mathcal{E}^* \times \mathcal{E}) = -\frac{b_1}{2\hbar} \mathbf{I} \cdot (\mathcal{E}' \times \mathcal{E}''), \quad (44)$$

is the vector component, and

$$\begin{aligned} \hat{H}_{\text{eff}(2)} &:= \frac{b_2}{4\hbar^2} \left[(\mathcal{E}^* \cdot \mathbf{I}) (\mathcal{E} \cdot \mathbf{I}) - \frac{1}{3} |\mathcal{E}|^2 \mathbf{I}^2 + \text{h.c.} \right] \\ &= \frac{b_2}{2\hbar^2} \left[(\mathcal{E}' \cdot \mathbf{I})^2 + (\mathcal{E}'' \cdot \mathbf{I})^2 - \frac{1}{3} |\mathcal{E}|^2 \mathbf{I}^2 \right], \end{aligned} \quad (45)$$

is the tensor component. In the above expressions, we used the real and imaginary parts of the complex light field $\mathcal{E} = \mathcal{E}' + i\mathcal{E}''$. This entirely analytical form allows one to explore its form to design desired atom-light coupling. Below we discuss three example configurations including a single beam and a pair of counter-propagating beams and a pair of perpendicular beams. The last configuration is demonstrated to generate spin-orbit coupling for the nuclear spin. Finally in Subsection IV D we discuss a way of eliminating the tensor light shifts by combining light fields with highly different frequencies.

A. Single beam

Let us consider first a situation where the system is subjected to a single linearly polarized laser beam

$$\mathcal{E} = \mathcal{E} e^{ikz} \mathbf{e}_z. \quad (46)$$

where the amplitude \mathcal{E} is assumed to be real and no extra global phase is added. This can be done by properly choosing the origin of spatial coordinates in all the examples considered here in Secs. IV A-IV C.

For the single beam the vector light shift (44) is zero and effective Hamiltonian contains only the position-independent scalar and tensor components

$$\hat{H}_{\text{eff}} = \frac{\mathcal{E}^2}{4} \left[b_0 \mathbb{1} + \frac{2b_2}{\hbar^2} \left(\mathbf{I}_z^2 - \frac{\mathbf{I}^2}{3} \right) \right], \quad (47)$$

where $\mathbb{1}$ is an identity operator. This shifts the ground-state energies according to $\hat{H}_{\text{eff}}|g\rangle|i_I, m_I\rangle = E_{m_I}^{(i_I)}|g\rangle|i_I, m_I\rangle$ with eigenvalues having a scalar term (independent of m_I) and tensor shifts (quadratic in m_I), namely $E_{m_I}^{(i_I)} = \mathcal{E}^2/4 [b_0 + 2b_2 (m_I^2 - \bar{i}_I^2/3)]$.

In the case of a circularly polarized laser beam,

$$\mathcal{E} = \mathcal{E} e^{ikz} \mathbf{e}_{\pm}, \quad \text{with } \mathbf{e}_{\pm} = \frac{1}{\sqrt{2}} (\mathbf{e}_x \pm i\mathbf{e}_y), \quad (48)$$

the effective Hamiltonian contains additionally the (position-independent) vector components $\propto \mathbf{I}_z$:

$$\hat{H}_{\text{eff}} = \frac{\mathcal{E}^2}{4} \left[b_0 \mathbb{1} \mp \frac{b_1}{\hbar} \mathbf{I}_z + \frac{b_2}{\hbar^2} \left(\frac{1}{3} \mathbf{I}^2 - \mathbf{I}_z^2 \right) \right]. \quad (49)$$

In this configuration, eigenenergies of the ground states manifold $|g\rangle|i_I, m_I\rangle$ contain additional position-independent linear (vector) shifts, $E_{m_I}^{(i_I)} = \mathcal{E}^2/4 [b_0 \mp b_1 m_I - b_2 (m_I^2 - \bar{i}_I^2/3)]$.

B. Two cross polarized counter-propagating laser beams

Consider next the effect of two cross-polarized counter-propagating Raman beams where

$$\mathcal{E} = \frac{\mathcal{E}^2}{\sqrt{2}} (e^{ikz} \mathbf{e}_x + e^{-ikz} \mathbf{e}_y). \quad (50)$$

In that case, the scalar light shift is uniform

$$\hat{H}_{\text{eff}(0)} = \frac{\mathcal{E}^2}{4} b_0 \mathbb{1} \quad (51)$$

and there are spatially periodic vector and tensor components

$$\hat{H}_{\text{eff}(1)} = \frac{\mathcal{E}^2}{4} \frac{b_1}{\hbar} \sin(2kz) \mathbf{I}_z. \quad (52)$$

and

$$\hat{H}_{\text{eff}(2)} = \frac{1}{2} \frac{b_2}{\hbar^2} \mathcal{E}^2 \left(\cos^2(kz) \mathbf{I}_y^2 + \sin^2(kz) \mathbf{I}_x^2 - \frac{1}{3} \mathbf{I}^2 \right), \quad (53)$$

with

$$\mathbf{I}_{\bar{x}} := \frac{\mathbf{I}_x - \mathbf{I}_y}{\sqrt{2}} \quad \text{and} \quad \mathbf{I}_{\bar{y}} := \frac{\mathbf{I}_x + \mathbf{I}_y}{\sqrt{2}}. \quad (54)$$

The latter $\hat{H}_{\text{eff}(2)}$ can be also represented in terms of the original nuclear spin operators $\mathbf{I}_{x,y,z}$:

$$\hat{H}_{\text{eff}(2)} = \frac{1}{2} \frac{b_2}{\hbar^2} \mathcal{E}^2 \left(\frac{1}{6} \mathbf{I}^2 - \frac{1}{2} \mathbf{I}_z^2 + \frac{\cos(2kz)}{2} \{\mathbf{I}_x, \mathbf{I}_y\} \right), \quad (55)$$

where anti-commutators can be rephrased by using the commutation relations: $\{\mathbf{I}_x, \mathbf{I}_y\} = [\mathbf{I}_y, \mathbf{I}_x] + 2\mathbf{I}_x \mathbf{I}_y = -i\hbar \mathbf{I}_z + 2\mathbf{I}_x \mathbf{I}_y$.

Therefore in addition to uniform position-independent light shifts, in this configuration involving counterpropagating light beams there is also a state-dependent periodic lattice potential due to the scalar and vector terms $\hat{H}_{\text{eff}(1)}$ and $\hat{H}_{\text{eff}(2)}$, Eqs. (52)-(55).

C. Two perpendicular light beams for spin orbit coupling

In the typical situations presented in the previous subsections, the effective Hamiltonian contains both vector and tensor shifts. Here we will consider a scheme in which these light shifts describe the spin-orbit coupling (SOC) of the NIST type [18, 23] supplied with an extra quadratic term (tensor light shift). For additional flexibility, we will allow a small frequency difference $\delta\omega$ with $|\delta\omega/A_{\text{HF}}| \ll 1$ between two beams enabling us to remove or modify the position-independent linear shift in the effective Hamiltonian.

The scheme involves two light beams of equal amplitudes propagating at a right angle. One of them is propagating along the z axis and is circularly \mathbf{e}_+ polarized. The second beam is propagating along the y axis with a linear polarization \mathbf{e}_z and a frequency difference $\delta\omega$ with respect to the first beam, so that

$$\mathcal{E} = \frac{\mathcal{E}}{\sqrt{2}} \left(\mathbf{e}_+ e^{ikz} + \mathbf{e}_z e^{i(ky - \delta\omega t)} \right). \quad (56)$$

The scalar light shift is then uniform, $\hat{H}_{\text{eff}(0)} = \frac{1}{4} b_0 \mathcal{E}^2$, and thus will be omitted by redefining the detuning energy Δ . The vector and tensor components are

$$\hat{H}_{\text{eff}(1)} = -\frac{\mathcal{E}^2}{8} \frac{b_1}{\hbar} \left(\mathbf{I}_z - \sqrt{2} \mathbf{I}_{xy}(s) \right), \quad (57)$$

$$\hat{H}_{\text{eff}(2)} = -\frac{\mathcal{E}^2}{4} \frac{b_2}{\hbar^2} \left(\frac{\mathbf{I}^2}{6} - \frac{\mathbf{I}_z^2}{2} - \frac{\{\mathbf{I}_{xy}(s), \mathbf{I}_z\}}{\sqrt{2}} \right), \quad (58)$$

where

$$\mathbf{I}_{xy}(s) := \mathbf{I}_x \cos(s) + \mathbf{I}_y \sin(s) \quad (59)$$

and $s = ky - kz - \delta\omega t$. Alternatively the operator $\mathbf{I}_{xy}(s)$ can be cast in terms of the spin raising and lowering operator $\mathbf{I}_{\pm} = \mathbf{I}_x \pm i\mathbf{I}_y$ as

$$\mathbf{I}_{xy}(s) = \mathbf{I}_+ e^{is} + \mathbf{I}_- e^{-is}. \quad (60)$$

The time dependence of linear and quadratic shifts can be eliminated by a unitary transformation describing the time-dependent spin rotation around the z axis

$$\hat{U} = \exp(-i\mathbf{I}_z \delta\omega t / \hbar). \quad (61)$$

Consequently $\mathbf{I}_{xy}(s)$ entering $\hat{H}_{\text{eff}(1)}$ and $\hat{H}_{\text{eff}(2)}$ transforms into the time-independent operator $\hat{U}^\dagger \mathbf{I}_{xy}(s) \hat{U} = \mathbf{I}_{xy}(ky - kz)$, and the light shifts take the form:

$$\hat{H}_{\text{eff}(1)} = -\frac{\mathcal{E}^2}{8} \frac{b_1}{\hbar} \left[\mathbf{I}_z - \sqrt{2} \mathbf{I}_{xy}(ky - kz) \right] + \delta\omega \mathbf{I}_z \quad (62)$$

and

$$\hat{H}_{\text{eff}(2)} = \frac{\mathcal{E}^2}{4} \frac{b_2}{\hbar^2} \left[-\frac{\mathbf{I}^2}{6} + \frac{\mathbf{I}_z^2}{2} + \frac{\{\mathbf{I}_{xy}(ky - kz), \mathbf{I}_z\}}{\sqrt{2}} \right], \quad (63)$$

where an extra linear Zeeman shift term $\delta\omega \mathbf{I}_z$ appears in $\hat{H}_{\text{eff}(1)}$ due to the time-dependence of the unitary transformation \hat{U} . In particular, by choosing $\delta\omega = b_1 \mathcal{E}^2 / 8\hbar$, the linear shift $\propto \mathbf{I}_z$ is eliminated in Eq. (62), giving

$$\hat{H}_{\text{eff}(1)} = \frac{\mathcal{E}^2}{4\sqrt{2}} \frac{b_1}{\hbar} \mathbf{I}_{xy}(ky - kz). \quad (64)$$

The operator $\mathbf{I}_{xy}(ky - kz)$ defined by Eq. (59) and featured in $\hat{H}_{\text{eff}(1)}$ and $\hat{H}_{\text{eff}(2)}$ represents the spin rotating in the xy plane when the atomic position changes in the $y-z$ direction. This provides a linear SOC of the NIST type

[18, 23] in the vector component of the effective Hamiltonian $\hat{H}_{\text{eff}(1)}$ given by Eqs. (62) or (64), and a more complex quadratic SOC in the tensor component $\hat{H}_{\text{eff}(2)}$ given by Eq. (63). Note that the position dependence of both linear and quadratic terms can be eliminated by an additional unitary operation $\hat{U}_1 = \exp[-i(kz - ky)\mathbf{I}_z/\hbar]$ transforming $\mathbf{I}_{xy}(ky - kz)$ to the position-independent spin operator \mathbf{I}_x . As in the case of spin-1/2 [18, 23], the SOC is then represented by the spin-dependent momentum shift when the atomic kinetic energy is included.

D. Combining significantly different frequencies for eliminating tensor light shifts

As exemplified above, realising purely linear light shifts, in particular the linear SOC, can be complicated for atoms with a large spin, as the tensor terms are present in typical configurations. It has been proposed to tune these out by stroboscopically alternating different polarisation configurations at a rate exceeding the atomic response rate [7]. As an alternative relying on continuous illumination, we propose to use a bichromatic light with two widely different frequencies, ensuring that the resulting vector light shifts are of the same sign. Yet, perfectly opposing tensor terms cancel each other.

In this way, let us consider two laser fields α and β with the same configurations, but significantly different detunings Δ_α and Δ_β . Specifically the frequency difference $\Delta_\alpha - \Delta_\beta$ should be large compared to the characteristic frequencies of the vector and tensor light shifts, so that the fast oscillating cross terms of the effective Hamiltonian average out. The resulting effective Hamiltonian is thus additive, namely is given by the sum of the effective Hamiltonians due to the separate fields α and β ,

$$\hat{H}_{\text{eff}} = \hat{H}_{\text{eff},\alpha} + \hat{H}_{\text{eff},\beta}. \quad (65)$$

In all situations considered in Secs. IV A-IV C, the linear and quadratic light shifts are characterised by the factors $\mathcal{E}^2 b_1 \equiv \mathcal{E}^2 b_1(\Delta)$ and $\mathcal{E}^2 b_2 \equiv \mathcal{E}^2 b_2(\Delta)$. For the bichromatic field these factors are to be replaced by $\mathcal{E}_\alpha^2 b_1(\Delta_\alpha) + \mathcal{E}_\beta^2 b_1(\Delta_\beta)$ and $\mathcal{E}_\alpha^2 b_2(\Delta_\alpha) + \mathcal{E}_\beta^2 b_2(\Delta_\beta)$, respectively, where the normalization condition $\mathcal{E}_\alpha^2 + \mathcal{E}_\beta^2 = 1$ applies to the amplitudes of the electric field. The quadratic light shift can be eliminated by properly choosing detunings and amplitudes of the electric fields such that $\mathcal{E}_\alpha^2 \text{Re}[b_2(\Delta_\alpha)] + \mathcal{E}_\beta^2 \text{Re}[b_2(\Delta_\beta)] = 0$.

The analytical expressions for the vector and tensor coefficients b_1 and b_2 make it easy to determine suitable configurations. In particular, we note that b_2 changes sign when crossing the central hyperfine line at $\Delta = E_{i_I}$, while b_1 does not (apart from a tiny spectral window), as one can see in Fig. 2 and 3. Thus one can eliminate the quadratic light shift by taking the detunings Δ_α and Δ_β to be on different sides of the central hyperfine line. For example, one can choose detunings to be symmetric with respect to the central hyperfine line: $\Delta_\alpha = E_{i_I} + \delta$

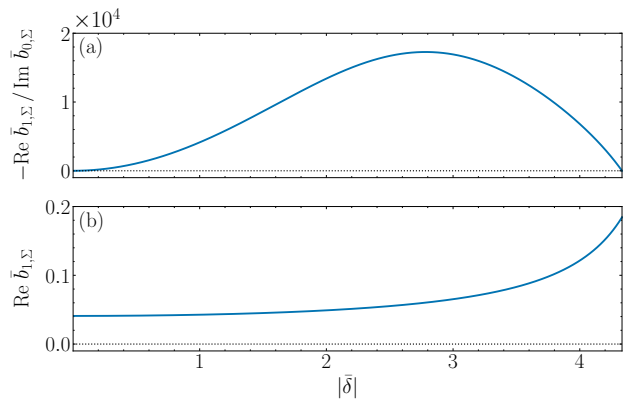


FIG. 4. The ratio $\text{Re } \bar{b}_{1,\Sigma} / \text{Im } \bar{b}_{0,\Sigma}$ (a, upper panel) and $\text{Re } \bar{b}_{1,\Sigma}$ (b, lower panel) vs the dimensionless detuning imbalance $\bar{\delta} = \delta / (\hbar A_{\text{HF}})$, where $\bar{b}_{i,\Sigma} = \mathcal{E}_\alpha^2 \bar{b}_i(\Delta_\alpha) + \mathcal{E}_\beta^2 \bar{b}_i(\Delta_\beta)$ (with $i=0,1,2$) are the dimensionless bichromatic coefficients. Here the normalization condition $\mathcal{E}_\alpha^2 + \mathcal{E}_\beta^2 = 1$ is used and the calculations were carried out for $\Gamma / |A_{\text{HF}}| \approx 3 \times 10^{-5}$. The amplitudes of bichromatic light beams were chosen such that the condition $\mathcal{E}_\alpha^2 \text{Re } \bar{b}_2(\Delta_\alpha) + \mathcal{E}_\beta^2 \text{Re } \bar{b}_2(\Delta_\beta) = 0$ holds, and the tensor light shift is eliminated. This requirement can be always satisfied for values of $\bar{\delta}$ shown in this plot, but not for arbitrary $\bar{\delta}$, as beyond this region signs of $\text{Re } \bar{b}_2(\Delta_\alpha)$ and $\text{Re } \bar{b}_2(\Delta_\beta)$ may become the same.

and $\Delta_\beta = E_{i_I} - \delta$ ³.

As shown in Fig. 4, for $i_I = 9/2$ corresponding to ^{87}Sr , at $\delta_{\text{optimal}} \simeq 3|A_{\text{HF}}|$ there is a local optimal ratio between vector shift and loss rate due to spontaneous emission, $\text{Re } \bar{b}_{1,\Sigma} / \text{Im } \bar{b}_{0,\Sigma}$, is 10^4 , where $\bar{b}_{i,\Sigma} = \mathcal{E}_\alpha^2 \bar{b}_i(\Delta_\alpha) + \mathcal{E}_\beta^2 \bar{b}_i(\Delta_\beta)$ (with $i=0,1,2$) are the dimensionless bichromatic coefficients.

Using two light fields even further detuned, away from the hyperfine structure, one can also have the opposite signs of b_2 and same signs of b_1 needed for the cancellation of the tensor light shifts without cancelling the vector ones. There are however two drawbacks: i) vector shifts smaller in absolute value, ii) a complication in the implementation of spin-dependent lattices or vector spin-orbit coupling. Indeed, the schemes considered in Sections IV B and IV C involve a local phase related to optical path differences between two beams. When superimposing two spin-dependent lattices created with light beams at differing wavelengths, the slight difference $k = k_\alpha - k_\beta$ in wavevectors k_α and k_β might matter. These difficulties can be overcome by working at the relatively small detuning within the hyperfine structure, as discussed above ($\delta_{\text{optimal}} \simeq 3|A_{\text{HF}}|$ for $i_I = 9/2$). In that case, one can ensure that the two polarization lattices are

³ The frequency difference δ in the bichromatic scheme should not be confused with a much smaller frequency difference $\delta\omega$ included in the scheme considered in Sec IV C to have an adjustable linear Zeeman shift.

in phase over the lengthscale of the atomic cloud. For example, in the counterpropagating beam configuration, where the optical path difference $2k(z - z_0)$ is typically controlled by the position z_0 of a mirror, this rephasing occurs every $z - z_0 = n \times \pi c/2\delta$ with $n \in \mathbb{N}$. For ^{87}Sr , one has $\pi c/2\delta_{\text{optimal}} \simeq 10$ cm. This is a macroscopic distance, so it is possible to tune the optical path length accurately enough and thus realize a good cancellation of the tensor light shift.

V. SUMMARY AND DISCUSSIONS

We have analyzed the effective Hamiltonian describing the scalar, vector, and tensor light shifts of nuclear spin states in alkaline earth atoms. Our approach, rooted in the Dyson identity, circumvents the need for explicit scrutiny of transitions within the excited state manifold's specific hyperfine states. Instead, we have derived simple analytical expressions for the coefficients defining the scalar, vector and tensor light shift in the effective Hamiltonian. Our work on one-body Hamiltonians can be a stepping stone to design experiments where ad-hoc one-body terms (such as SOC) combined with interatomic interactions lead to emerging phenomena (quan-

tum phases, spintronic applications).

We have explored typical examples of light configurations capable of inducing light shifts for the nuclear spin states in the ground electronic state manifold. Additionally, we have discerned configurations governing SOC that encompass both linear and quadratic shifts, alongside those characterized by purely linear SOC effects.

The breadth of our analytical findings is broad-reaching and can be applied to other alkaline earth (or alkaline earth-like) atoms with analogous structures. We anticipate that the straightforward analytical expressions for scalar, vector, and tensor terms we have provided will prove helpful in guiding future experimental endeavours and fostering a more profound theoretical comprehension of systems subjected to off-resonance light coupling.

ACKNOWLEDGMENTS

We gratefully acknowledge discussions with Bruno Laburthe-Tolra. This work was supported by DAINA project of the Polish National Science Center UMO-2020/38/L/ST2/00375 and Lithuanian Research Council S-LL-21-3. E.W. acknowledges support of the Polish National Science Centre project UMO-2016/22/E/ST3/00045.

Appendix A: Dyson equation/identity

Let us consider a Hamiltonian represented in terms of the zero-order Hamiltonian H_0 and the interaction operator V as: $H = H_0 + V$. We define the full Green operator $G = (\Delta - H)^{-1}$ and the zero-order Green operator $G_0 = (\Delta - H_0)^{-1}$, where Δ is some parameter in energy units; in the present situation it is the detuning. The Green operator obeys the Dyson equation (identity)

$$G = G_0 + G_0 V G. \quad (\text{A1})$$

The validity of the Dyson identity can be proved by rearranging the Green operator in the following way:

$$G = G_0(\Delta - H_0)G = G_0(\Delta - H + V)G = G_0 + G_0 V G. \quad (\text{A2})$$

The Dyson equation (A1) is exact and valid for any H_0 and V , no approximation or assumption has been made. Note also that in this work we take $H_0 = 0$ and $V = H_{\text{HF}}$. In that case, Eq. (A1) reduces to Dyson equation presented in the main text in Eq. (13).

Appendix B: Derivation of the the equation for \mathbf{K} and its solution

1. Equation for \mathbf{K}

The vector operator \mathbf{K} with the Cartesian components K_i is defined as

$$K_s = D_{s,q} \mathcal{E}_q, \quad (\text{B1})$$

where $D_{s,q}$ is a tensor describing the second order light induced interaction for the ground state atoms:

$$D_{s,q} = P_g d_s P_e G P_e d_q P_g. \quad (\text{B2})$$

Applying the Dyson identity for G given by Eq. (13) or (A1), one gets the following relation for $D_{s,q}$:

$$D_{s,q} = \frac{|d_{ge}^2|}{\Delta} P_g \delta_{sq} + P_g d_s P_e H_{\text{HF}} G P_e d_q P_g. \quad (\text{B3})$$

Combining it with the expression (B1) for \mathbf{K} , one has:

$$\mathbf{K} = \frac{1}{\Delta} P_g |d_{ge}^2| \boldsymbol{\mathcal{E}} + \frac{A_{\text{HF}}}{\hbar \Delta} P_g \mathbf{d} P_e (\mathbf{I} \cdot \mathbf{J}) \left(1 + \frac{\gamma}{\hbar^2} \mathbf{I} \cdot \mathbf{J} \right) G P_e (\mathbf{d} \cdot \boldsymbol{\mathcal{E}}) P_g. \quad (\text{B4})$$

Our aim is get a closed equation [Eq. (B17)] for \mathbf{K} containing only the spin operators \mathbf{I} and the electric field amplitude $\boldsymbol{\mathcal{E}}$. For this, we will carry out the following steps. Since \mathbf{J} commutes with P_e and gives zero when acting on the ground state manifold ($P_g \mathbf{J} = 0$), one has

$$P_g d_i P_e (\mathbf{J} \cdot \mathbf{I}) = P_g d_i (\mathbf{J} \cdot \mathbf{I}) P_e = P_g [d_i, (\mathbf{J} \cdot \mathbf{I})] P_e = -i\hbar \epsilon_{lik} P_g d_k P_e I_l, \quad (\text{B5})$$

where the use has been made of the commutator relations [24]:

$$[J_i, d_j] = [L_i, d_j] = i\hbar \epsilon_{ijk} d_k, \quad (\text{B6})$$

Equation (B5) can be represented in a vector form as:

$$P_g \mathbf{d} P_e (\mathbf{J} \cdot \mathbf{I}) = i\hbar P_g \mathbf{I} \times \mathbf{d} P_e. \quad (\text{B7})$$

With this Eq. (B4) reduces to

$$\mathbf{K} = \frac{1}{\Delta} P_g |d_{ge}^2| \boldsymbol{\mathcal{E}} + i \frac{A_{\text{HF}}}{\Delta} P_g \left[\mathbf{I} \times \mathbf{d} P_e + \frac{\gamma}{\hbar^2} (\mathbf{I} \times \mathbf{d}) P_e (\mathbf{I} \cdot \mathbf{J}) \right] G P_e (\mathbf{d} \cdot \boldsymbol{\mathcal{E}}) P_g. \quad (\text{B8})$$

Using the commutation relation (B6), one has for the Cartesian components of the operator $P_g (\mathbf{I} \times \mathbf{d}) P_e (\mathbf{I} \cdot \mathbf{J})$:

$$P_g (\mathbf{I} \times \mathbf{d})_i P_e (\mathbf{I} \cdot \mathbf{J}) = \epsilon_{ilk} I_l P_g d_k P_e (\mathbf{I} \cdot \mathbf{J}) = i\hbar \epsilon_{ilk} \epsilon_{kpq} I_l P_g d_q P_e I_p. \quad (\text{B9})$$

Since $\epsilon_{ilk} \epsilon_{kpq} = \epsilon_{ilk} \epsilon_{pqk} = \delta_{ip} \delta_{lq} - \delta_{iq} \delta_{lp}$, then

$$P_g (\mathbf{I} \times \mathbf{d})_i P_e (\mathbf{I} \cdot \mathbf{J}) = i\hbar P_g (I_l d_l I_i - I_l d_i I_l) P_e = i\hbar P_g (I_i I_l d_l - d_i I_l I_l) P_e - \hbar^2 \epsilon_{ikl} I_k P_g d_l P_e. \quad (\text{B10})$$

In vector form this reads:

$$P_g (\mathbf{I} \times \mathbf{d}) P_e (\mathbf{I} \cdot \mathbf{J}) = i\hbar P_g [\mathbf{I} (\mathbf{I} \cdot \mathbf{d}) - \mathbf{I}^2 \mathbf{d}] P_e - \hbar^2 P_g (\mathbf{I} \times \mathbf{d}) P_e. \quad (\text{B11})$$

Therefore, the relation (B8) transforms to

$$\mathbf{K} = \frac{1}{\Delta} P_g |d_{ge}^2| \boldsymbol{\mathcal{E}} + i \frac{A_{\text{HF}}}{\Delta} P_g \left[(1 - \gamma) (\mathbf{I} \times \mathbf{d}) + i \frac{\gamma}{\hbar} (\mathbf{I} (\mathbf{I} \cdot \mathbf{d}) - \mathbf{I}^2 \mathbf{d}) \right] P_e G P_e (\mathbf{d} \cdot \boldsymbol{\mathcal{E}}) P_g. \quad (\text{B12})$$

The final step is to form the operator \mathbf{K} from \mathbf{d} and G in Eq. (B12). Using Eqs. (B1) and (B2), one can write

$$P_g d_i G P_e (\mathbf{d} \cdot \boldsymbol{\mathcal{E}}) P_g = P_g d_i P_e G P_e d_u P_g \mathcal{E}_u = D_{iu} \mathcal{E}_u = K_i. \quad (\text{B13})$$

Equivalently in the vector form one has

$$P_g \mathbf{d} P_e G P_e (\mathbf{d} \cdot \boldsymbol{\mathcal{E}}) P_g = \mathbf{K}. \quad (\text{B14})$$

Analogously, the following relations hold:

$$P_g (\mathbf{I} \times \mathbf{d}) P_e G P_e (\mathbf{d} \cdot \boldsymbol{\mathcal{E}}) P_g = \mathbf{I} \times \mathbf{K}, \quad (\text{B15})$$

$$P_g (\mathbf{I} \cdot \mathbf{d}) P_e G P_e (\mathbf{d} \cdot \boldsymbol{\mathcal{E}}) P_g = \mathbf{I} \cdot \mathbf{K}. \quad (\text{B16})$$

Hence the relation (B12) provides the required equation for \mathbf{K} :

$$\eta \mathbf{K} = \frac{1}{\Delta} P_g |d_{ge}^2| \boldsymbol{\mathcal{E}} + i \frac{A_{\text{HF}}}{\Delta} (1 - \gamma) (\mathbf{I} \times \mathbf{K}) - \gamma \frac{A_{\text{HF}}}{\hbar \Delta} \mathbf{I} (\mathbf{I} \cdot \mathbf{K}), \quad (\text{B17})$$

where

$$\eta = 1 - \gamma A_{\text{HF}} \hbar i_I (i_I + 1) / \Delta. \quad (\text{B18})$$

2. Solution of equation for \mathbf{K}

As explained in the main text, we are looking for the solution of Eq. (B17) in the form

$$\mathbf{K} = \left[a_0 \boldsymbol{\mathcal{E}} - i \frac{a_1}{\hbar} \mathbf{I} \times \boldsymbol{\mathcal{E}} + \frac{a_2}{\hbar^2} \mathbf{I} (\mathbf{I} \cdot \boldsymbol{\mathcal{E}}) \right] P_g, \quad (\text{B19})$$

Substituting this ansatz into Eq. (B17), one finds

$$\eta \mathbf{K} = \frac{1}{\Delta} P_g |d_{ge}^2| \boldsymbol{\mathcal{E}} + i \frac{A_{\text{HF}}}{\Delta} (1 - \gamma) P_g \left[a_0 \mathbf{I} \times \boldsymbol{\mathcal{E}} - i \frac{a_1}{\hbar} \mathbf{I} \times (\mathbf{I} \times \boldsymbol{\mathcal{E}}) + \frac{a_2}{\hbar^2} \mathbf{I} \times \mathbf{I} (\mathbf{I} \cdot \boldsymbol{\mathcal{E}}) \right] + \mathbf{K}_\gamma, \quad (\text{B20})$$

where

$$\mathbf{K}_\gamma = -\gamma \frac{A_{\text{HF}}}{\hbar \Delta} \mathbf{I} (\mathbf{I} \cdot \mathbf{K}) = -\gamma \frac{A_{\text{HF}}}{\hbar \Delta} P_g \mathbf{I} \left[a_0 (\mathbf{I} \cdot \boldsymbol{\mathcal{E}}) - i \frac{a_1}{\hbar} \mathbf{I} \cdot (\mathbf{I} \times \boldsymbol{\mathcal{E}}) + \frac{a_2}{\hbar^2} (\mathbf{I} \cdot \mathbf{I}) (\mathbf{I} \cdot \boldsymbol{\mathcal{E}}) \right]. \quad (\text{B21})$$

The above relation can be rewritten as

$$\mathbf{K}_\gamma = -\gamma \frac{A_{\text{HF}}}{\hbar \Delta} P_g \left[a_0 + a_1 + a_2 \frac{\mathbf{I}^2}{\hbar^2} \right] \mathbf{I} (\mathbf{I} \cdot \boldsymbol{\mathcal{E}}), \quad (\text{B22})$$

where we used cyclic commutation relations for the components of the nuclear spin operator \mathbf{I} , that gives $\mathbf{I} \times \mathbf{I} = i\hbar \mathbf{I}$ (a general property of quantum angular momenta operators), and also the relation $\mathbf{I} \cdot (\mathbf{I} \times \boldsymbol{\mathcal{E}}) = \boldsymbol{\mathcal{E}} \cdot (\mathbf{I} \times \mathbf{I}) = i\hbar \mathbf{I} \cdot \boldsymbol{\mathcal{E}}$.

Rearranging the vector operators entering the r.h.s. of Eq. (B20), one has

$$\eta \mathbf{K} = \frac{1}{\Delta} P_g |d_{ge}^2| \boldsymbol{\mathcal{E}} + i \frac{A_{\text{HF}}}{\Delta} (1 - \gamma) P_g \left[(a_0 + a_1) \mathbf{I} \times \boldsymbol{\mathcal{E}} + \frac{i}{\hbar} (-a_1 + a_2) \mathbf{I} (\mathbf{I} \cdot \boldsymbol{\mathcal{E}}) + i \frac{a_1}{\hbar} \boldsymbol{\mathcal{E}} \mathbf{I}^2 \right] + \mathbf{K}_\gamma, \quad (\text{B23})$$

where in the term proportional to a_2 relation $\mathbf{I} \times \mathbf{I} = i\hbar \mathbf{I}$ was applied, while in the term proportional to a_1 the calculation is as follows:

$$(\mathbf{I} \times (\mathbf{I} \times \boldsymbol{\mathcal{E}}))_k = \epsilon_{kij} \epsilon_{mnp} I_i I_m \mathcal{E}_n = I_i \mathcal{E}_i I_k - I_i I_i \mathcal{E}_k = I_k I_i \mathcal{E}_i - I_i I_i \mathcal{E}_k + i\hbar \epsilon_{ikl} \mathcal{E}_l I_l = I_k (\mathbf{I} \cdot \boldsymbol{\mathcal{E}}) - \mathcal{E}_k \mathbf{I}^2 + i\hbar (\mathbf{I} \times \boldsymbol{\mathcal{E}})_k. \quad (\text{B24})$$

Putting to Eq. (B23) the expression (B22) for \mathbf{K}_γ and grouping terms proportional to $\boldsymbol{\mathcal{E}}$, $\mathbf{I} \times \boldsymbol{\mathcal{E}}$ and $\mathbf{I} (\mathbf{I} \cdot \boldsymbol{\mathcal{E}})$, the following equation is obtained

$$\begin{aligned} \eta \Delta \cdot \mathbf{K} = & \left[|d_{ge}^2| - A_{\text{HF}} (1 - \gamma) \mathbf{I}^2 \frac{a_1}{\hbar} \right] \boldsymbol{\mathcal{E}} P_g + \frac{i}{\hbar} \left[\hbar A_{\text{HF}} (1 - \gamma) (a_0 + a_1) \right] \mathbf{I} \times \boldsymbol{\mathcal{E}} P_g + \\ & + \frac{1}{\hbar^2} \left[A_{\text{HF}} \hbar \left((1 - \gamma) (a_1 - a_2) - \gamma \left(a_0 + a_1 + \frac{\mathbf{I}^2}{\hbar^2} a_2 \right) \right) \right] \mathbf{I} (\mathbf{I} \cdot \boldsymbol{\mathcal{E}}) P_g. \end{aligned} \quad (\text{B25})$$

Substituting Eq. (B19) into (B25) and comparing the factors at terms proportional to $\boldsymbol{\mathcal{E}}$, $\mathbf{I} \times \boldsymbol{\mathcal{E}}$ and $\mathbf{I} (\mathbf{I} \cdot \boldsymbol{\mathcal{E}})$, one arrives at the following closed set of equations for the coefficients a_0 , a_1 and a_2 :

$$\eta \Delta a_0 = |d_{ge}^2| - A_{\text{HF}} (1 - \gamma) \mathbf{I}^2 \frac{a_1}{\hbar}, \quad (\text{B26})$$

$$\eta \Delta a_1 = -\hbar A_{\text{HF}} (1 - \gamma) (a_0 + a_1), \quad (\text{B27})$$

$$\eta \Delta a_2 = \hbar A_{\text{HF}} \left[(1 - \gamma) (a_1 - a_2) - \gamma \left(a_0 + a_1 + \frac{\mathbf{I}^2}{\hbar^2} a_2 \right) \right]. \quad (\text{B28})$$

The solution of this system of equations reads

$$a_0 = \frac{|d_{ge}^2| (\Delta + \hbar A_{\text{HF}} (1 - \gamma) (\mathbf{I}^2 / \hbar^2 + 1))}{(\Delta - E_{i_{l+1}}) (\Delta - E_{i_{l-1}})}, \quad (\text{B29})$$

$$a_1 = -\frac{\hbar A_{\text{HF}} |d_{ge}^2| (1 - \gamma)}{(\Delta - E_{i_{l+1}}) (\Delta - E_{i_{l-1}})}, \quad (\text{B30})$$

$$a_2 = -\frac{\hbar A_{\text{HF}} |d_{ge}^2| [\hbar A_{\text{HF}} + \gamma (\Delta - 2\hbar A_{\text{HF}}) - \gamma^2 \hbar A_{\text{HF}} (\mathbf{I}^2 / \hbar^2 - 1)]}{(\Delta - E_{i_{l+1}}) (\Delta - E_{i_l}) (\Delta - E_{i_{l-1}})}, \quad (\text{B31})$$

where E_{i_l} and $E_{i_{l\pm 1}}$ featured in denominators are eigenenergies given by Eqs. (4)-(6) The numerators can also be represented in terms of eigenenergies, as in Eqs. (22)-(24) of the main text.

Appendix C: A Clebsch-Gordan approach for calculating effective Hamiltonian

Throughout this paper, we used the Dyson equation method for calculating the Green operator and thus the effective Hamiltonian. The method has the advantage of being analytically solvable and providing a physical intuition. Here, we summarize another method, a commonly used Clebsch-Gordan approach which works well for numerical analysis but is not convenient for analytics. The calculations based on the Clebsch-Gordan approach will then be compared with the ones based on the Dyson equation approach.

We are interested in the effective Hamiltonian \hat{H}_{eff} describing the light-induced coupling between the atomic nuclear spin states in the ground electronic state manifold. It is given by Eqs. (10)-(12) in the main text, i.e.

$$\hat{H}_{\text{eff}} = \frac{1}{4} \mathcal{E}_s^* D_{s,q} \mathcal{E}_q, \quad (\text{C1})$$

where:

$$D_{s,q} = P_g d_s P_e G P_e d_q P_g, \quad \text{with } G = (\Delta - H_{\text{HF}})^{-1}. \quad (\text{C2})$$

Here P_g and P_e are unit projector operators onto the ground state (1S_0) and excited state (3P_1) manifolds, respectively. In the latter 3P_1 manifold the eigenstates of the hyperfine Hamiltonian H_{HF} are $|j_e i_I f m_f\rangle$, where $j_e = 1$ is electron total angular momentum and $i_I - 1 \leq f \leq i_I + 1$ is the total angular momentum of the atom. The corresponding hyperfine energies E_f are given by Eqs. (4) and (6) in the main text. The Green operator projected onto this excited state manifold is diagonal in the basis of eigenstates $|j_e i_I f m_f\rangle$ and reads explicitly:

$$P_e G P_e = \sum_{f=i_I-j_e}^{i_I+j_e} \sum_{m_f=-f}^f \frac{|j_e i_I f m_f\rangle \langle j_e i_I f m_f|}{\Delta - E_f}. \quad (\text{C3})$$

Expressing hyperfine eigenstates $|j_e i_I f m_f\rangle$ in terms of the bare electron and spin states $|j_e i_I m_{j_e} m_i\rangle \equiv |j_e m_{j_e}\rangle |i_I m_i\rangle$ via the Clebsch-Gordan coefficients $C_{j_e i_I m_{j_e} m_i}^{f m_f}$, one has

$$P_e G P_e = \sum_{m_j, m_i, m'_j, m'_i, f, m_f} |j_e m_{j_e}\rangle |i_I m_i\rangle \frac{C_{j_e i_I m_{j_e} m_i}^{f m_f} C_{j_e i_I m'_{j_e} m'_i}^{f m_f*}}{\Delta - E_f} \langle j_e m'_{j_e} | \langle i_I m'_i |. \quad (\text{C4})$$

Finally, since the dipole operator acts only on the electronic degrees of freedom, Eq. (C2) for the tensor $D_{s,q}$ takes the form:

$$D_{s,q} = P_g \sum_{m_i, m'_i} |i_I m_i\rangle D_{s,q}^{m_i, m'_i} \langle i_I m'_i |, \quad (\text{C5})$$

with

$$D_{s,q}^{m_i, m'_i} = \sum_{m_j, m'_j, f, m_f} \langle j_g m_{j_g} | d_s | j_e m_j \rangle \frac{C_{j_e i_I m_{j_e} m_i}^{f m_f} C_{j_e i_I m'_{j_e} m'_i}^{f m_f*}}{\Delta - E_f} \langle j_e m'_{j_e} | d_q | j_g m'_{j_g} \rangle, \quad (\text{C6})$$

where $j_g = 0$ and $m_{j_g} = 0$ are, respectively, the electron angular momentum and its projection quantum numbers for the ground state manifold 1S_0 , and the unit projection operator onto this manifold is $P_g = |j_g m_{j_g}\rangle \langle j_g m_{j_g}|$.

We now define the dipole moment matrix elements $\langle j_g m_{j_g} | d_s | j_e m_j \rangle \equiv \langle ^1S_0 | d_s | ^3P_1, m_j \rangle$ featured in Eq. (C6). As discussed in ref. [25] (chapt. 3 p. 50, chapt. 10 p. 350-351), if we identify the two-photon polarisation states $|\sigma^\pm\rangle$ to photon angular momentum states $|j = 1, m = \pm 1\rangle$, and defining the photon angular momentum operator \vec{J} , the states must transform as $\exp\{-i\pi J_y\} |\sigma^+\rangle = +|\sigma^-\rangle$ to satisfy the standard raising and lowering operator conventions. The commonly used relations between circular and linear polarization states $|\sigma^\pm\rangle = (|x\rangle \pm i|y\rangle)/\sqrt{2}$ do not satisfy that, and will lead to erroneous tensorial shift calculations. Instead one must use $|\sigma^\pm\rangle = (\mp|x\rangle - i|y\rangle)/\sqrt{2}$. Consequently, the matrix elements of the atomic dipole operators $d_{x,y,z} = \vec{d} \cdot \vec{e}_{x,y,z}$ are

$$\langle ^1S_0 | d_x | ^3P_1, m_j \rangle = \frac{d_{ge}}{\sqrt{2}} (\delta_{m_j, -1} - \delta_{m_j, 1}), \quad (\text{C7})$$

$$\langle {}^1S_0 | d_y | {}^3P_1, m_j \rangle = -\frac{d_{ge}}{i\sqrt{2}} (\delta_{m_j,1} + \delta_{m_j,-1}), \quad (\text{C8})$$

$$\langle {}^1S_0 | d_z | {}^3P_1, m_j \rangle = d_{ge} \delta_{m_j,0}. \quad (\text{C9})$$

Using Eqs. (C1), (C5)-(C6) and (C7)-(C9), the matrix elements of the effective Hamiltonian were numerically calculated and compared with analytical results in Fig. 2 showing a perfect agreement between numerical and analytical results.

-
- [1] A. J. Daley, M. M. Boyd, J. Ye, and P. Zoller, Quantum Computing with Alkaline-Earth-Metal Atoms, *Phys. Rev. Lett.* **101**, 170504 (2008).
- [2] D. González-Cuadra, D. Bluvstein, M. Kalinowski, R. Kaubuegger, N. Maskara, P. Naldesi, T. V. Zache, A. M. Kaufman, M. D. Lukin, H. Pichler, B. Vermersch, J. Ye, and P. Zoller, Fermionic quantum processing with programmable neutral atom arrays, *Proceedings of the National Academy of Sciences* **120**, 10.1073/pnas.2304294120 (2023).
- [3] Q. Li, C. Mukhopadhyay, and A. Bayat, Fermionic simulators for enhanced scalability of variational quantum simulation, *Phys. Rev. Res.* **5**, 043175 (2023).
- [4] A. V. Gorshkov, A. M. Rey, A. J. Daley, M. M. Boyd, J. Ye, P. Zoller, and M. D. Lukin, Alkaline-Earth-Metal Atoms as Few-Qubit Quantum Registers, *Phys. Rev. Lett.* **102**, 110503 (2009).
- [5] J. W. Lis, A. Senoo, W. F. McGrew, F. Rönchen, A. Jenkins, and A. M. Kaufman, Midcircuit Operations Using the omg Architecture in Neutral Atom Arrays, *Phys. Rev. X* **13**, 041035 (2023).
- [6] S. Omanakuttan, A. Mitra, M. J. Martin, and I. H. Deutsch, Quantum optimal control of ten-level nuclear spin qubits in ${}^{87}\text{Sr}$, *Phys. Rev. A* **104**, L060401 (2021).
- [7] M. A. Perlin, D. Barberena, M. Mamaev, B. Sundar, R. J. Lewis-Swan, and A. M. Rey, Engineering infinite-range $SU(n)$ interactions with spin-orbit-coupled fermions in an optical lattice, *Phys. Rev. A* **105**, 023326 (2022).
- [8] J. J. McFerran, D. V. M. aes, C. Mandache, J. Millo, W. Zhang, Y. L. Coq, G. Santarelli, and S. Bize, Laser locking to the 199Hg $1S_0$ - $3P_0$ clock transition with $5.4 \times 10^{-15} / \sqrt{\tau}$ fractional frequency instability, *Opt. Lett.* **37**, 3477 (2012).
- [9] A. Yamaguchi, M. S. Safronova, K. Gibble, and H. Katori, Narrow-line Cooling and Determination of the Magic Wavelength of Cd, *Phys. Rev. Lett.* **123**, 113201 (2019).
- [10] G. Wang and A. Ye, Possibility of using Zn as the quantum absorber for a laser-cooled neutral atomic optical frequency standard, *Phys. Rev. A* **76**, 043409 (2007).
- [11] A. Derevianko and H. Katori, Colloquium: Physics of optical lattice clocks, *Rev. Mod. Phys.* **83**, 331 (2011).
- [12] V. A. Dzuba and A. Derevianko, Blackbody radiation shift for the 1S_0 - 3P_0 optical clock transition in zinc and cadmium atoms, *Journal of Physics B: Atomic, Molecular and Optical Physics* **52**, 215005 (2019).
- [13] A. D. Ludlow, M. M. Boyd, J. Ye, E. Peik, and P. O. Schmidt, Optical atomic clocks, *Rev. Mod. Phys.* **87**, 637 (2015).
- [14] S. Chaudhury, S. Merkel, T. Herr, A. Silberfarb, I. H. Deutsch, and P. S. Jessen, Quantum Control of the Hyperfine Spin of a Cs Atom Ensemble, *Phys. Rev. Lett.* **99**, 163002 (2007).
- [15] P. Rosenbusch, S. Ghezali, V. A. Dzuba, V. V. Flambaum, K. Beloy, and A. Derevianko, ac Stark shift of the Cs microwave atomic clock transitions, *Phys. Rev. A* **79**, 013404 (2009).
- [16] I. H. Deutsch and P. S. Jessen, Quantum control and measurement of atomic spins in polarization spectroscopy, *Optics Communications* **283**, 681 (2010).
- [17] F. Le Kien, P. Schneeweiss, and A. Rauschenbeutel, Dynamical polarizability of atoms in arbitrary light fields: general theory and application to cesium, *The European Physical Journal D* **67**, 92 (2013).
- [18] N. Goldman, G. Juzeliūnas, P. Öhberg, and I. B. Spielman, Light-induced gauge fields for ultracold atoms, *Reports on Progress in Physics* **77**, 126401 (2014).
- [19] H. Miyake, N. C. Pimenti, P. K. Elgee, A. Sitarum, and G. K. Campbell, Isotope-shift spectroscopy of the ${}^1S_0 \rightarrow {}^3P_1$ and ${}^1S_0 \rightarrow {}^3P_0$ transitions in strontium, *Phys. Rev. Res.* **1**, 033113 (2019).
- [20] C. J. Foot, *Atomic physics*, Vol. 7 (OUP Oxford, 2004).
- [21] G. zu Putlitz, Bestimmung des elektrischen Kernquadrupolmomentes des ungeraden stabilen Strontium-87-Kerns, *Zeitschrift für Physik* **175**, <https://doi.org/10.1007/BF01375346> (1963).
- [22] T. Hernández Yanes, M. Płodzień, M. Mackoīt Sinkevičienė, G. Žlabys, G. Juzeliūnas, and E. Witkowska, One- and Two-Axis Squeezing via Laser Coupling in an Atomic Fermi-Hubbard Model, *Physical Review Letters* **129**, 10.1103/physrevlett.129.090403 (2022).
- [23] Y.-J. Lin, K. Jiménez-García, and I. B. Spielman, Spin-orbit-coupled Bose-Einstein condensates, *Nature* **471**, 83 (2011).
- [24] L. D. Landau and L. M. Lifshitz, *Quantum Mechanics Non-Relativistic Theory, Third Edition: Volume 3* (1981).
- [25] M. Le Bellac and A. Bers, *Physique quantique (1ere edition)* (EDP sciences, 2003).